



# Functional Characterization of an Interferon Gamma Receptor-Like Protein on *Entamoeba histolytica*

Julieta Pulido-Ortega,<sup>a</sup> Patricia Talamás-Rohana,<sup>b</sup> Martín Humberto Muñoz-Ortega,<sup>c</sup> Liseth Rubí Aldaba-Muruato,<sup>d</sup> Sandra Luz Martínez-Hernández,<sup>a</sup> María del Rosario Campos-Esparza,<sup>a</sup> Daniel Cervantes-García,<sup>e</sup> Aralia Leon-Coria,<sup>f</sup> France Moreau,<sup>f</sup> Kris Chadee,<sup>f</sup>  Javier Ventura-Juárez<sup>a</sup>

<sup>a</sup>Departamento de Morfología, Centro de Ciencias Básicas, Universidad Autónoma de Aguascalientes, Aguascalientes, Ags., Mexico

<sup>b</sup>Departamento de Infectómica y Patogénesis Molecular, Centro de Investigación y de Estudios Avanzados del Instituto Politécnico Nacional, Mexico City, Mexico

<sup>c</sup>Departamento de Química, Centro de Ciencias Básicas, Universidad Autónoma de Aguascalientes, Aguascalientes, Ags., Mexico

<sup>d</sup>Unidad Académica Multidisciplinaria Zona Huasteca, Universidad Autónoma de San Luis Potosí, San Luis Potosí, S.L.P., Mexico

<sup>e</sup>CONACYT-Departamento de Microbiología, Centro de Ciencias Básicas, Universidad Autónoma de Aguascalientes, Aguascalientes, Ags., Mexico

<sup>f</sup>Department of Microbiology, Immunology and Infectious Diseases, Snyder Institute for Chronic Diseases, Cumming School of Medicine, University of Calgary, Calgary, Alberta, Canada

**ABSTRACT** *Entamoeba histolytica* is an anaerobic parasitic protozoan and the causative agent of amoebiasis. *E. histolytica* expresses proteins that are structurally homologous to human proteins and uses them as virulence factors. We have previously shown that *E. histolytica* binds exogenous interferon gamma (IFN- $\gamma$ ) on its surface, and in this study, we explored whether exogenous IFN- $\gamma$  could modulate parasite virulence. We identified an IFN- $\gamma$  receptor-like protein on the surface of *E. histolytica* trophozoites by using anti-IFN- $\gamma$  receptor 1 (IFN- $\gamma$ R1) antibody and performing immunofluorescence, Western blot, protein sequencing, and *in silico* analyses. Coupling of human IFN- $\gamma$  to the IFN- $\gamma$  receptor-like protein on live *E. histolytica* trophozoites significantly upregulated the expression of *E. histolytica* cysteine protease A1 (*EhCP-A1*), *EhCP-A2*, *EhCP-A4*, *EhCP-A5*, amebapore A (APA), cyclooxygenase 1 (*Cox-1*), Gal-lectin (*Hgl*), and peroxiredoxin (*Prx*) in a time-dependent fashion. IFN- $\gamma$  signaling via the IFN- $\gamma$  receptor-like protein enhanced *E. histolytica*'s erythrophagocytosis of human red blood cells, which was abrogated by the STAT1 inhibitor fludarabine. Exogenous IFN- $\gamma$  enhanced chemotaxis of *E. histolytica*, its killing of Caco-2 colonic and Hep G2 liver cells, and amebic liver abscess formation in hamsters. These results demonstrate that *E. histolytica* expresses a surface IFN- $\gamma$  receptor-like protein that is functional and may play a role in disease pathogenesis and/or immune evasion.

**KEYWORDS** *Entamoeba histolytica*, amoebiasis, cysteine proteases, IFN- $\gamma$ , erythrophagocytosis, cytopathic effect

**E***ntamoeba histolytica* infects the human large intestine, causing amoebiasis, dysentery, and in advanced cases, amoebic liver abscesses, leading to ~55,000 deaths annually (1). Studies on the host-parasite relationship have established that *E. histolytica* has developed strategies to escape from host immune responses (2–5). This phenomenon is known as positive natural selection, which drives the increase in prevalence of advantageous traits, and it has played a central role in the development of *E. histolytica* as a human parasite (6). On the other hand, it could be taken as coevolution at the biochemical level, defined as the process of reciprocal, adaptive genetic change between interacting species (7). In the colon, *E. histolytica* trophozoites overcome innate host defenses with molecules such as cysteine proteases to degrade mucus (8) and prostaglandin E<sub>2</sub> (PGE<sub>2</sub>) to stimulate epithelial cells to produce interleukin-8 (IL-8),

**Citation** Pulido-Ortega J, Talamás-Rohana P, Muñoz-Ortega MH, Aldaba-Muruato LR, Martínez-Hernández SL, Campos-Esparza MDR, Cervantes-García D, Leon-Coria A, Moreau F, Chadee K, Ventura-Juárez J. 2019. Functional characterization of an interferon gamma receptor-like protein on *Entamoeba histolytica*. *Infect Immun* 87:e00540-19. <https://doi.org/10.1128/IAI.00540-19>.

**Editor** DeBroski R. Herbert, University of Pennsylvania

**Copyright** © 2019 Pulido-Ortega et al. This is an open-access article distributed under the terms of the [Creative Commons Attribution 4.0 International license](https://creativecommons.org/licenses/by/4.0/).

Address correspondence to Kris Chadee, [kchadee@ucalgary.ca](mailto:kchadee@ucalgary.ca), or Javier Ventura-Juárez, [jventur@correo.uaa.mx](mailto:jventur@correo.uaa.mx).

**Received** 15 July 2019

**Accepted** 7 August 2019

**Accepted manuscript posted online** 19 August 2019

**Published** 18 October 2019

a chemoattractant for neutrophils (9). Various virulence factors act on different stages of the invasion process, such as Gal/GalNAc lectin for adhesion to host cells (10), amebapores that cause cytolysis of immune cells (11), and cysteine proteases that degrade mucins (12) and immunoglobulins like IgA (13) and cause tissue destruction (14).

The ability of *E. histolytica* trophozoites to survive in the host has been related in part to the remarkable mobility of surface antigens after interaction with antibodies, which leads to elimination of the resulting antigen-antibody complexes by capping (15). *E. histolytica* trophozoites can protect themselves from reactive oxygen species (ROS) produced by neutrophils with peroxiredoxin, a 29-kDa surface protein that has potent antioxidant activity (16, 17). In addition, *E. histolytica* trophozoites express a protein similar to CD59 on the cell membrane that prevents the polymerization of complement protein C9 (18). *E. histolytica* also expresses a 55-kDa protein, similar to the extracellular loop of human occludin, which allows it to bind to intestinal epithelial cells (19). Furthermore, through bioinformatics analysis, two proteins, a GTPase of the Rab family and a thioredoxin containing a TIR-like domain similar to those of the IL-1 receptor and human Toll-like receptors (TLRs), have been identified (20). Reports have also shown that *E. histolytica* trophozoites bind the inflammatory cytokine IL-8 through a 29-kDa membrane-associated protein, triggering chemotaxis of the parasites to the source of IL-8 (21). *In vitro* chemotaxis assays, utilizing gradients of tumor necrosis factor alpha (TNF- $\alpha$ ), have shown that *E. histolytica* is attracted toward the source of this cytokine (22).

Previous studies have shown that interferon gamma (IFN- $\gamma$ ) binds on the surface of *E. histolytica* and reduces protein and DNA synthesis in cultured *E. histolytica* trophozoites (23). We have shown that *E. histolytica* trophozoites derived from colonic tissues from fulminant amoebic colitis patients are highly positive for IFN- $\gamma$  (24) and speculated that *E. histolytica* has a surface binding protein for this cytokine. In this study, we demonstrate that IFN- $\gamma$  coupling to *E. histolytica* IFN- $\gamma$  receptor-like protein upregulated virulence factors that enhanced phagocytosis, cytopathic effects on colonic and liver cells, and liver abscess formation in a hamster model.

## RESULTS

**Detection of IFN- $\gamma$  on *E. histolytica*.** IFN- $\gamma$  plays an important role in host defense against *E. histolytica* by activating macrophages to produce ROS and nitrogen species that are cytotoxic to the parasite (16). With the use of a highly specific anti-human IFN- $\gamma$  monoclonal antibody, we detected by immunofluorescence increasing amounts of IFN- $\gamma$ -antibody complexes on the surface of *E. histolytica* trophozoites at 60 and 180 min of exposure (Fig. 1A). To support the specific recognition of IFN- $\gamma$ , a Western blot analysis was performed under reducing conditions that identified a 17-kDa protein corresponding to IFN- $\gamma$  localized on the membrane of *E. histolytica* trophozoites (Fig. 1B). As a positive control, an antibody against the Gal/GalNAc lectin (4) was used to confirm the localization of IFN- $\gamma$  on the *E. histolytica* membrane (Fig. 1B).

To quantify the localization of IFN- $\gamma$  to the putative receptor on the surface of *E. histolytica* trophozoites, parasites were incubated with anti-human IFN- $\gamma$ R1 monoclonal antibody and anti-IFN- $\gamma$  polyclonal antibody and binding quantified by immunofluorescence. Surprisingly, we observed for both antibodies (anti-IFN- $\gamma$ R1 and anti-IFN- $\gamma$  antibodies) strong signals as early as 20 min that increased in intensity after 180 min (Fig. 2A) toward the uroid end of the *E. histolytica* trophozoites (Fig. 2B, white arrow). Colocalization of IFN- $\gamma$  and anti-human IFN- $\gamma$ R1 antibody on trophozoites was highest after 60 min of interaction with IFN- $\gamma$  (Fig. 2C). To corroborate the results obtained by confocal microscopy, membrane proteins from trophozoites were separated by SDS-PAGE (12%) and subjected to Western blotting with a monoclonal antibody against IFN- $\gamma$ R1 (trophozoites were incubated for 20 min with recombinant human IFN- $\gamma$ ). As a positive control, the antibody recognized IFN- $\gamma$ R1 in human leukocyte lysates at 50 kDa (Fig. 3, lane 1). Our results suggest that *E. histolytica* trophozoites express a membrane protein of approximately 200 kDa that is recognized by anti-human IFN- $\gamma$ R1 antibody

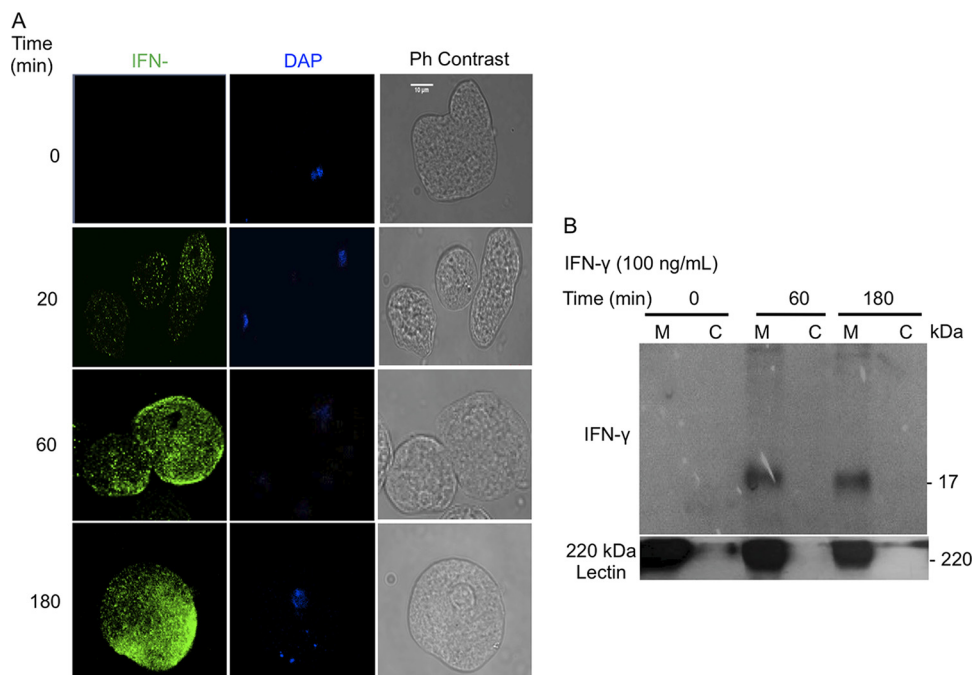


**FIG 1** Localization of IFN- $\gamma$  on the surface of *E. histolytica* trophozoites. (A) Immunodetection of the IFN- $\gamma$  protein on the surface of *E. histolytica* trophozoites incubated with anti-human IFN- $\gamma$  antibody (1:100 dilution), followed by a secondary antibody conjugated to Alexa 488 (1:1,000), imaged by confocal microscopy. Note that the intense green staining is absent in the control (without IFN- $\gamma$ ) at time zero. Ph contrast, phase-contrast images. (B) Western blot detection of the 17-kDa protein corresponding to IFN- $\gamma$  on *E. histolytica* membrane (M) and cytoplasmic (C) fractions at 60 and 180 min. The 220-kDa lectin was used as an internal control to confirm membrane localization and subcellular fractionation. Scale bar represents 10  $\mu$ m.

independently of whether the trophozoites are exposed to exogenous IFN- $\gamma$  or not (Fig. 3). These results suggest that *E. histolytica* expresses an IFN- $\gamma$  receptor-like molecule on its surface that binds exogenous IFN- $\gamma$  on the surface of the parasite.

**Mass spectrometry analysis.** To identify the 200-kDa protein, extracts of *E. histolytica* membranes were separated by SDS-PAGE and stained with Coomassie blue. The 200-kDa protein was then excised and analyzed by mass spectrometry (MS). Peptide analysis revealed four proteins in the *E. histolytica* proteome that matched with different scores (Fig. 4A). The putative surface antigen C4LTV2\_ENTHI, reported as a putative tyrosine kinase, showed the highest match and percent coverage in comparison with the protein with the expected molecular weight of approximately 200 kDa (Fig. 4B). These peptides cover 28.6% of the amebic 200-kDa-protein sequence reported as a putative tyrosine kinase. Due to the high score and other features of the C4LTV2\_ENTHI sequence, our results indicate a high possibility that the anti-IFN- $\gamma$ R1 antibody detected the amebic protein in the Western blot and is most likely the putative tyrosine kinase. Further investigation of this possibility showed (Fig. 4C) that the human IFN- $\gamma$ R1 amino acid sequence has an ETTTCYIRVYNVYVRMNGSEIQYKILTQKE DDCDEIQCQLAIPVSSLNSQYC motif in the third extracellular loop, characterized as a binding site for IL-8, which aligns with the NTYCDVCEENYIIIDGTCYFRAINKCESSDGIK TKCSSGYTPKGYC motif of the 200-kDa amebic surface antigen (putative tyrosine kinase), sharing identical amino acids at 10 specific positions, while the other 20 amino acids, although not identical, have similar physicochemical properties.

**IFN- $\gamma$  upregulates the expression of *E. histolytica* virulence factors.** Reverse transcriptase quantitative PCR was performed to determine if exposure of live *E. histolytica* trophozoites to IFN- $\gamma$  could modulate the transcription of key virulence factors in *E. histolytica* cells. After 20 min of exposure to IFN- $\gamma$ , *E. histolytica* cysteine protease A1 (*EhCP-A1*), *EhCP-A2*, *EhCP-A4*, and *EhCP-A5* mRNAs were significantly increased compared to their levels in control *E. histolytica* trophozoites in the absence of

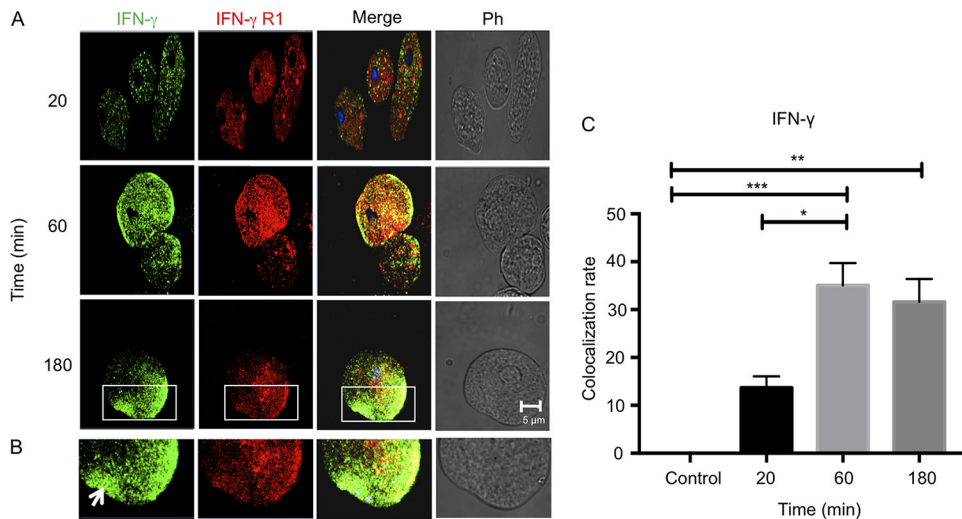


**FIG 2** Colocalization of IFN- $\gamma$  and IFN- $\gamma$  receptor-like protein on *E. histolytica* trophozoites. *E. histolytica* trophozoites were incubated with IFN- $\gamma$  for 20, 60, or 180 min and analyzed by confocal microscopy. After the interaction, trophozoites were incubated with a polyclonal anti-IFN- $\gamma$  antibody (1:100 dilution) and a monoclonal anti-IFN- $\gamma$ R1 antibody (1:100 dilution), followed by Alexa Fluor 594- and Alexa Fluor 488-labeled secondary antibodies, respectively. (A) Micrographs show that IFN- $\gamma$  bound to the surface of *E. histolytica* trophozoites; an increase in positive signal was obtained with longer exposure time. The label for IFN- $\gamma$  receptor-like protein was constant after 3 h of interaction and was displaced to the uroid side of trophozoites. Increased colocalization at 1 h of interaction was observed. (B) Images illustrating morphology that demonstrate capping (arrow) on an *E. histolytica* trophozoite after interaction with IFN- $\gamma$  for 3 h. Ph, phase-contrast images. (C) Analysis was performed according to the Costes methodology, which includes the elimination of autofluorescence with the Coloc2 plugin of Fiji software (ImageJ). The graph was made with GraphPad Prism 7. \*,  $P < 0.05$ ; \*\*,  $P < 0.01$ ; \*\*\*,  $P < 0.001$ .

IFN- $\gamma$ . The fold increases were highest for *EhCP-A1* and *EhCP-A5* (20- and 39-fold, respectively) (Fig. 5A and D). *E. histolytica* amebapore A (*APA*), cyclooxygenase 1 (*Cox-1*), and peroxiredoxin (*Prx*) mRNAs were significantly increased, by 16-fold, after 30 min of exposure (Fig. 6A and B). The mRNA expression of both *Prx* (20-fold) and Gal-lectin (*Hgl*) (17-fold) peaked after 60 min (Fig. 6C and D).

**Pretreating *E. histolytica* trophozoites with IFN- $\gamma$  increases erythrophagocytosis.** One of the properties of *E. histolytica* is its extraordinary phagocytic activity against a variety of particulate materials, including bacteria, sloughed epithelial cells, and erythrocytes. The latter activity has been widely accepted as a characteristic presented by invasive *E. histolytica* (25). For this reason, we determined whether IFN- $\gamma$  enhanced erythrophagocytosis in *E. histolytica* trophozoites. IFN- $\gamma$  pretreatment for 20 min significantly increased trophozoite phagocytosis of red blood cells (Fig. 7A), which was specifically abrogated by the phospho-STAT1 inhibitor fludarabine (Fig. 7B). These results indicate that IFN- $\gamma$  promoted erythrophagocytosis when it bound to *E. histolytica* trophozoites through the IFN- $\gamma$  receptor-like protein, possibly by activating STAT1. Accordingly, we next investigated whether IFN- $\gamma$ -stimulated *E. histolytica* phosphorylated STAT1. To investigate this, we immunoprecipitated *E. histolytica* proteins with phospho-tyrosine and performed Western blotting with phospho-STAT1 under the conditions shown in Fig. 7B. Surprisingly, the basal expression (nonstimulated controls) of phospho-STAT1 in *E. histolytica* trophozoites was similar to that in IFN- $\gamma$ -stimulated trophozoites, and pretreatment with the phospho-STAT1 inhibitor fludarabine (50  $\mu$ M) markedly decreased phospho-STAT1 (Fig. 7C). The viability of *E. histolytica* trophozoites treated with 50 mM fludarabine was >95% as determined by the trypan blue exclusion assay. Lower concentrations of fludarabine (10 and 25 nM) were not effective in inhibiting basal IFN- $\gamma$ -stimulated phospho-STAT1. These results demonstrate that basal expression of STAT1 in *E. histolytica* trophozoites was constitutively high and that STAT1 could not be phosphorylated further with IFN- $\gamma$ . However, under both conditions, fludarabine markedly inhibited the phosphorylation of STAT1 (Fig. 7C).

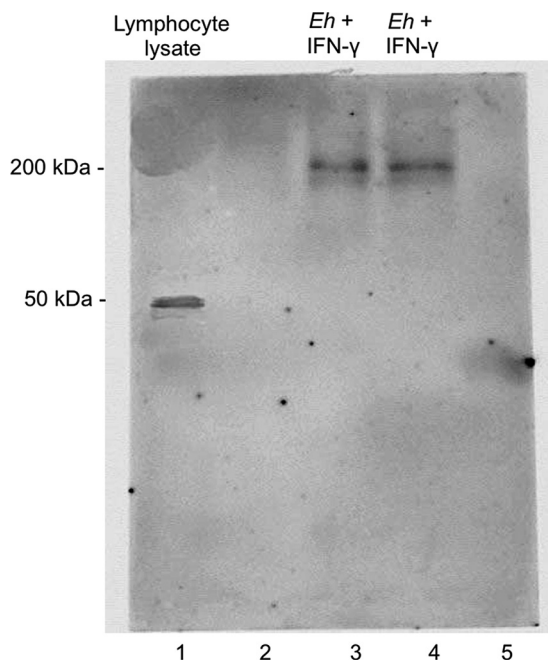


**FIG 3** Western blot of *E. histolytica* membrane fractions using anti-human IFN- $\gamma$ R1 antibody. *E. histolytica* proteins were analyzed by 12% SDS-PAGE and immunoblotting. *E. histolytica* trophozoites were incubated with or without 100 ng/ml IFN- $\gamma$ . Note strong immunoreactivity with the anti-IFN- $\gamma$ R1 antibody at 200 kDa in *E. histolytica* membrane fractions (lanes 3 and 4) and at 50 kDa in lymphocyte lysate used as controls (lane 1). Lanes 2 and 5 are blanks.

**Pretreating *E. histolytica* trophozoites with IFN- $\gamma$  increases chemotaxis.** Chemotaxis is a phenomenon in which cells direct their movements according to the presence of certain chemical substances in the environment. *E. histolytica* orients its migration or chemotaxis based on external stimuli like serum proteins, bacteria, or molecules released by epithelial and immune cells (26), such as IL-8 (21). This activity in *E. histolytica* has been correlated with its invasive capacity (21, 27). Chemotaxis requires specific recognition between the chemoattractant and the receptor on the cell, leading to a series of activation signals that induce biochemical and structural changes that allow migration. *E. histolytica* trophozoites exposed to 100 ng/ml of IFN- $\gamma$  showed a significant increase in migration that was 4 times greater (Fig. 8Ac and Fig. 8B) than the migration of untreated control trophozoites in medium only (Fig. 8Aa and Fig. 8B; Movie S1 in the supplemental material). For these studies, IL-8 was used as a positive control (Fig. 8Ab) and cytochalasin D, an inhibitor of actin cytoskeleton, as a negative control (Fig. 8Ad). Chemotaxis of *E. histolytica* was also analyzed by time-lapse video. For each recording in real time, a representative *E. histolytica* trophozoite was selected for each condition, and their trajectories were followed throughout 4 min (Movies S1 and S2).

**IFN- $\gamma$  increases *E. histolytica*'s cytopathic activity toward Caco-2 and HepG2 cells.** The ability of *E. histolytica* trophozoites to destroy target cells can be separated into two phases: recognition and adhesion, which allows cell death and phagocytosis (28). To determine if IFN- $\gamma$  pretreatment increased *E. histolytica*'s cytopathic activity, studies were carried out using human colonic Caco2 and liver HepG2 cell monolayers. After 20 min of interaction with IFN- $\gamma$ , *E. histolytica* trophozoites had destroyed a greater percentage of the HepG2 monolayer (Fig. 9B) than of the Caco-2 cells (Fig. 9A), and the Caco-2 cell destruction was partially inhibited by the STAT1 inhibitor fludarabine. Shorter incubation times with IFN- $\gamma$  and the STAT1 inhibitor had no effect on *E. histolytica*'s cytopathic activity.

**In vivo effect of stimulating *E. histolytica* trophozoites with IFN- $\gamma$ .** We next tested whether treating *E. histolytica* with IFN- $\gamma$  affected the morphological develop-



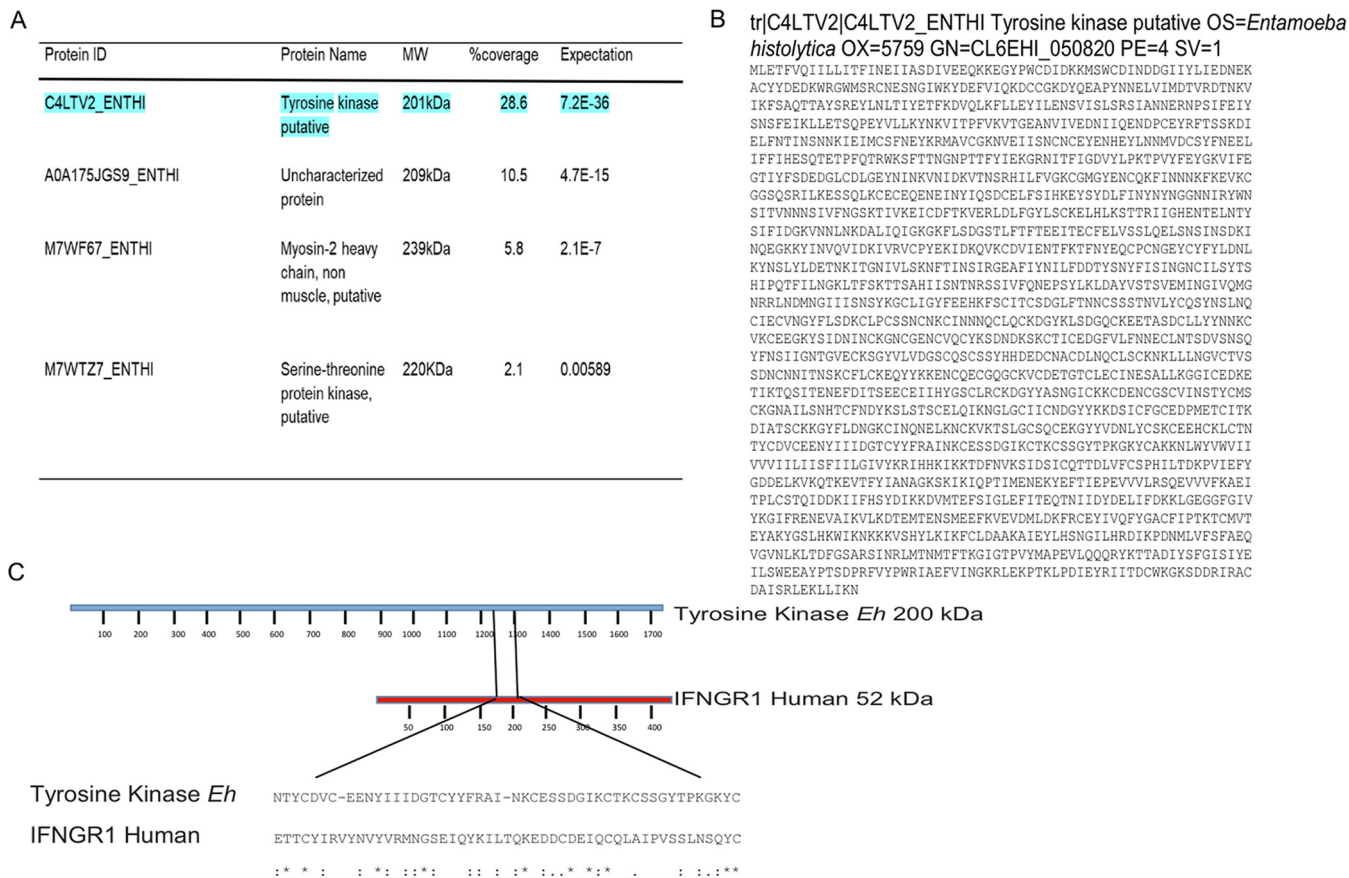


**FIG 4** Analysis of the anti-human IFN- $\gamma$ R1 antibody detected a 200-kDa amebic protein. (A) Analysis of the 200-kDa-protein band by mass spectrometry (MS) identified four *E. histolytica* proteins by peptide analysis. The highlighted protein at the top of the list is reported as a putative amebic surface antigen and as a putative tyrosine kinase of *E. histolytica*. (B) Sequence of the reported *E. histolytica* 200-kDa surface antigen (putative tyrosine kinase). (C) Alignment of IFN- $\gamma$ R1 human amino acid sequence and *E. histolytica* 200-kDa surface antigen (putative tyrosine kinase). The similar amino acid motifs, with 20% identity between the two proteins, are flanked by slanted lines. Ten of the amino acids in this motif are identical, and the other 20 have similar physicochemical properties.

ment of amebic liver abscesses (ALA) in hamsters. Hamsters were inoculated with  $5 \times 10^5$  *E. histolytica* trophozoites pretreated or not with IFN- $\gamma$  for 20 min. Livers of animals inoculated with untreated trophozoites showed the characteristic ALA lesions produced after 4 days, which were small and white and localized to the site of inoculation in the left liver lobe (Fig. 10B, arrows). In marked contrast, ALA produced by trophozoites pretreated with IFN- $\gamma$ , but not by trophozoites treated with IFN- $\gamma$  and anti-IFN- $\gamma$  antibody, produced several granulomas that were distributed throughout the left liver lobe, with a few metastatic foci in other liver lobes (Fig. 10C and D). By histopathology, the lesions produced by untreated trophozoites and trophozoites treated with IFN- $\gamma$  and anti-IFN- $\gamma$  antibody showed characteristic ALA granulomas that had a central necrotic region with edges of intense inflammatory infiltrates bordering healthy liver tissues (Fig. 11A and B). The lesions produced by *E. histolytica* trophozoites pretreated with IFN- $\gamma$  (Fig. 11C) show significantly larger areas of necrosis (Fig. 11D), with several peripheral small granulomas (Fig. 11C, yellow arrows). By immunohistochemistry, trophozoites are readily seen at the periphery of the lesions (Fig. 12A and B, yellow arrows), and in lesions caused by trophozoites pretreated with IFN- $\gamma$ , trophozoites were found in the lesion walls and in close proximity to healthy liver tissues (Fig. 12C, inset, yellow arrow).

**DISCUSSION**

In the host-parasite interactions between *E. histolytica* trophozoites and human tissues, the mechanisms that trigger *E. histolytica* invasion are poorly understood. Our

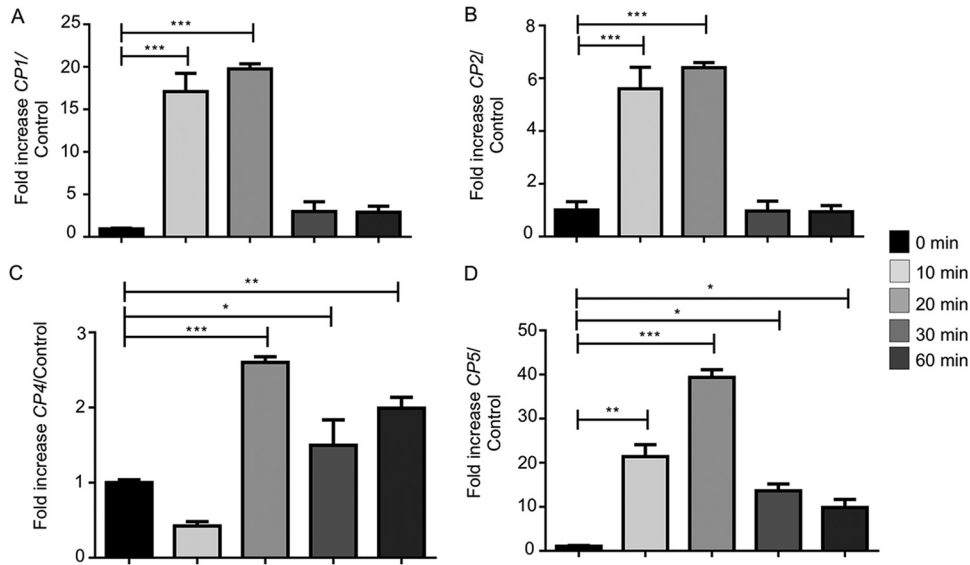


**FIG 5** IFN- $\gamma$  upregulated cysteine protease expression in *E. histolytica* trophozoites. (A to D) *E. histolytica* trophozoites treated or not with IFN- $\gamma$  for 10, 20, 30, or 60 min showed increased expression of cysteine protease genes associated with *E. histolytica* pathogenicity. Note maximal upregulation of *EhCP-A1*, *EhCP-A2*, *EhCP-A4*, and *EhCP-A5* expression after 20 min of IFN- $\gamma$  stimulation. \*,  $P < 0.05$ ; \*\*,  $P < 0.01$ ; \*\*\*,  $P < 0.001$ .

study reveals that *E. histolytica* has a surface protein analogous to human IFN- $\gamma$  receptor 1 (IFN- $\gamma$ R1) and responds to the presence of IFN- $\gamma$  to modify its behavior/virulence. In particular, IFN- $\gamma$  activated *E. histolytica* trophozoites to upregulate the expression of virulence genes *EhCP-A1*, *EhCP-A2*, *EhCP-A4*, *EhCP-A5*, *APA*, *Prx*, *Hgl*, and *Cox-1*. These findings are remarkable and lend support to the idea that *E. histolytica* uses IFN- $\gamma$  in tissues to sense inflammatory/immune cells so as to enhance invasion and/or evade immune responses. As IFN- $\gamma$  is present at sites of *E. histolytica* invasion, in the presence of inflammatory macrophages and T cells, evading the immune response by upregulating cysteine proteases to degrade cytokines might be the most likely scenario. *E. histolytica* avoids the host immune response through

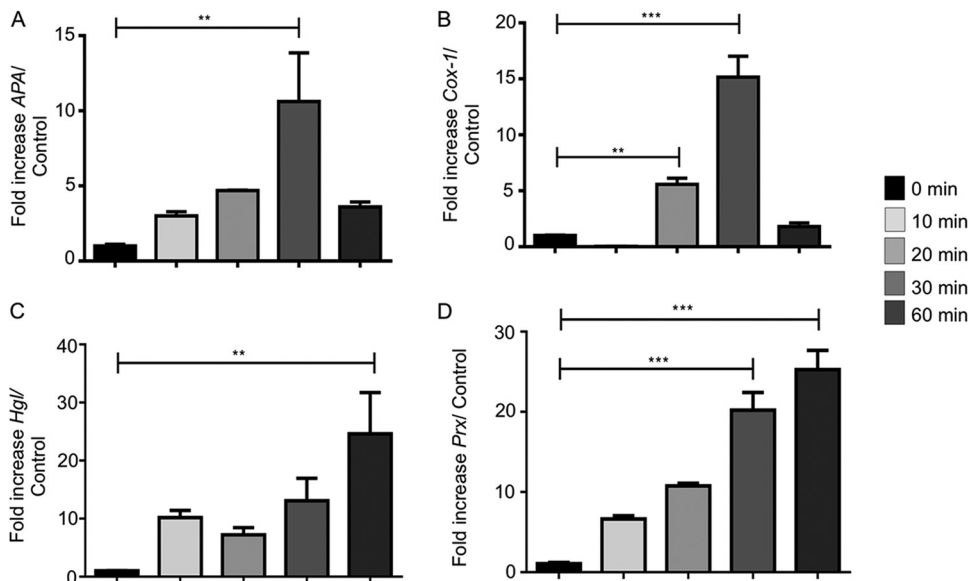


**FIG 6** IFN- $\gamma$  upregulated other virulence genes in *E. histolytica* in a temporal fashion. (A to D) Interaction of *E. histolytica* trophozoites with IFN- $\gamma$  upregulated *APA*, *Cox-1*, *Hgl*, and *Prx* (peroxiredoxin), with maximal expression occurring after 30 min. \*,  $P < 0.05$ ; \*\*,  $P < 0.01$ ; \*\*\*,  $P < 0.001$ .

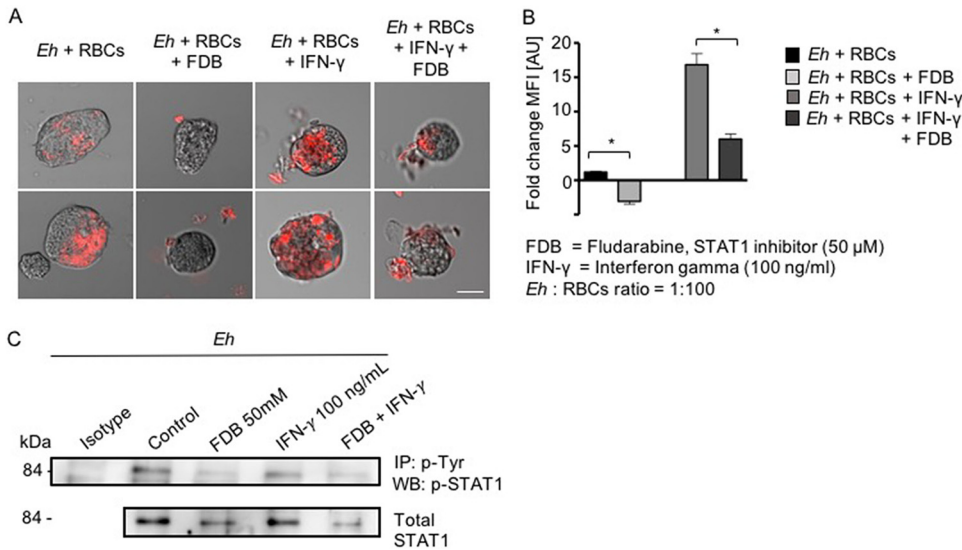


**FIG 7** IFN- $\gamma$  enhanced erythrophagocytosis in *E. histolytica* trophozoites. (A) Images of erythrophagocytosis by nontreated *E. histolytica* trophozoites (*Eh*) or by trophozoites in the presence of fludarabine or IFN- $\gamma$  or both. Note that IFN- $\gamma$ -stimulated erythrophagocytosis was substantially inhibited with the STAT1 inhibitor fludarabine. Red fluorescence shows ingested erythrocytes. Scale bar represents 10  $\mu$ m. (B) Histogram showing quantification of the fluorescence of erythrocytes phagocytosed in the different assays. MFI, mean fluorescence intensity; AU, arbitrary units. \*,  $P < 0.05$ . (C) Basal and IFN- $\gamma$ -induced phosphorylation of STAT1 in *E. histolytica* is inhibited by the phospho-STAT1 inhibitor fludarabine. IP, immunoprecipitation; WB, Western blotting.

adherence, cytotoxicity, or phagocytosis of inflammatory cells to downregulate immune effector cells and by degrading antibodies and complement with an arsenal of molecules, including amebapores, adhesins, phospholipases, serine-rich proteins, and lipopeptidophosphoglycan-like molecules (29–31). In addition, *E. histolytica* produces inhibiting factors that modulate immune cell function, includ-

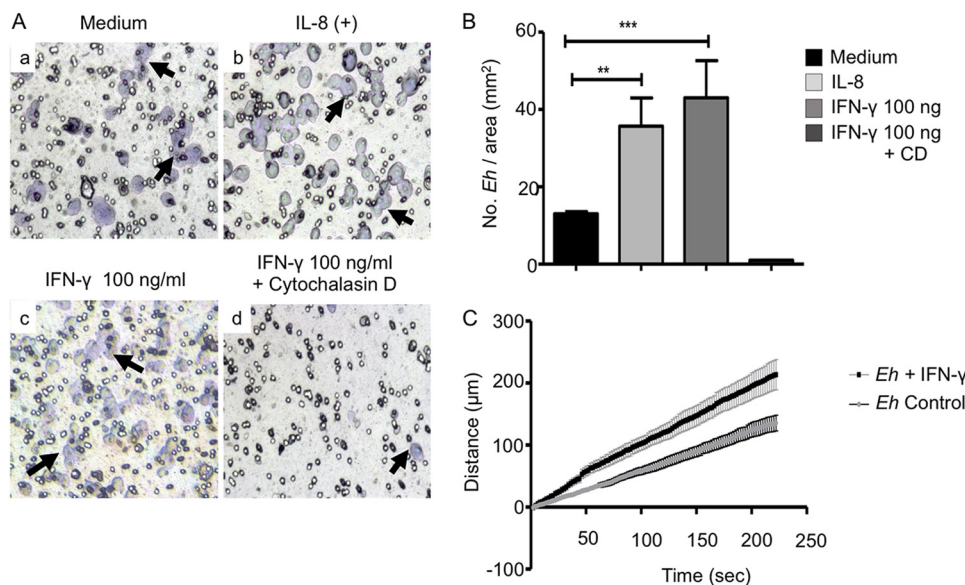


**FIG 8** Chemotaxis of *E. histolytica* trophozoites toward human IFN- $\gamma$ . (A) Microscopy images of *E. histolytica* trophozoites that were deposited in the upper chambers of Transwell units and allowed to migrate to the lower chambers in the absence (a) or presence (c) of IFN- $\gamma$  or in the presence of IL-8 as a positive migration control (b) or of IFN- $\gamma$  in the presence of 10  $\mu$ g/ml of cytochalasin D (d). Arrows indicate *E. histolytica* trophozoites. (B) Numbers of *E. histolytica* trophozoites/mm<sup>2</sup>. Data represent values from four independent experiments. CD, cytochalasin D. (C) *E. histolytica* trophozoite velocities tracked in the presence or absence of IFN- $\gamma$ . The graph represents migration velocities recorded by real-time video microscopy. \*\*,  $P < 0.01$ ; \*\*\*,  $P < 0.001$ .



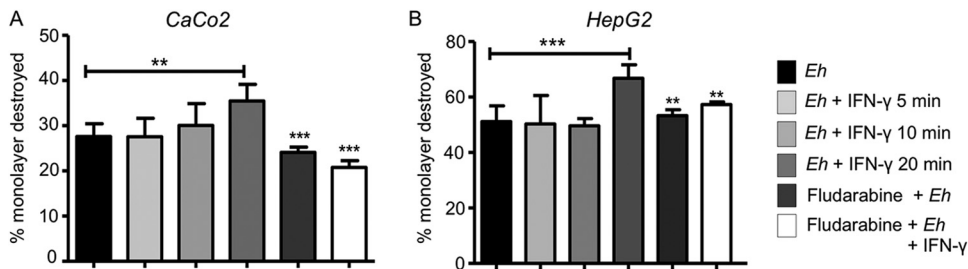


**FIG 9** IFN- $\gamma$  enhanced *E. histolytica*'s cytopathic effects on Caco-2 and HepG2 cells. (A, B) Caco-2 cells (A) and HepG2 cell monolayers (B) were exposed to *E. histolytica* trophozoites pretreated with IFN- $\gamma$  at different times with or without the STAT1 inhibitor fludarabine (50  $\mu$ M). Following interaction with *E. histolytica*, the remaining cells were stained with methylene blue and the released color measured at 655 nm. Data represent values from 4 independent experiments. \*\*,  $P < 0.01$ ; \*\*\*,  $P < 0.001$ .

ing a monocyte locomotion inhibitory factor that prevents chemotaxis and the activation of macrophages (32). *E. histolytica* also produces L220, which stimulates macrophages to produce IL-10 (33), and a specific parasite-encoded cytokine, *E. histolytica* MIF, as a mediator of mucosal inflammation (34).

During amebic invasion in the colon, *E. histolytica* trophozoites are highly positive for IFN- $\gamma$  located in the submucosa at sites where macrophages,  $\gamma\delta$  T cells, and NK cells are actively producing IFN- $\gamma$  (35). IFN- $\gamma$  activates macrophages and neutrophils that kill *E. histolytica* *in vitro* (35, 36), and high levels of IFN- $\gamma$  have been related to resistance to

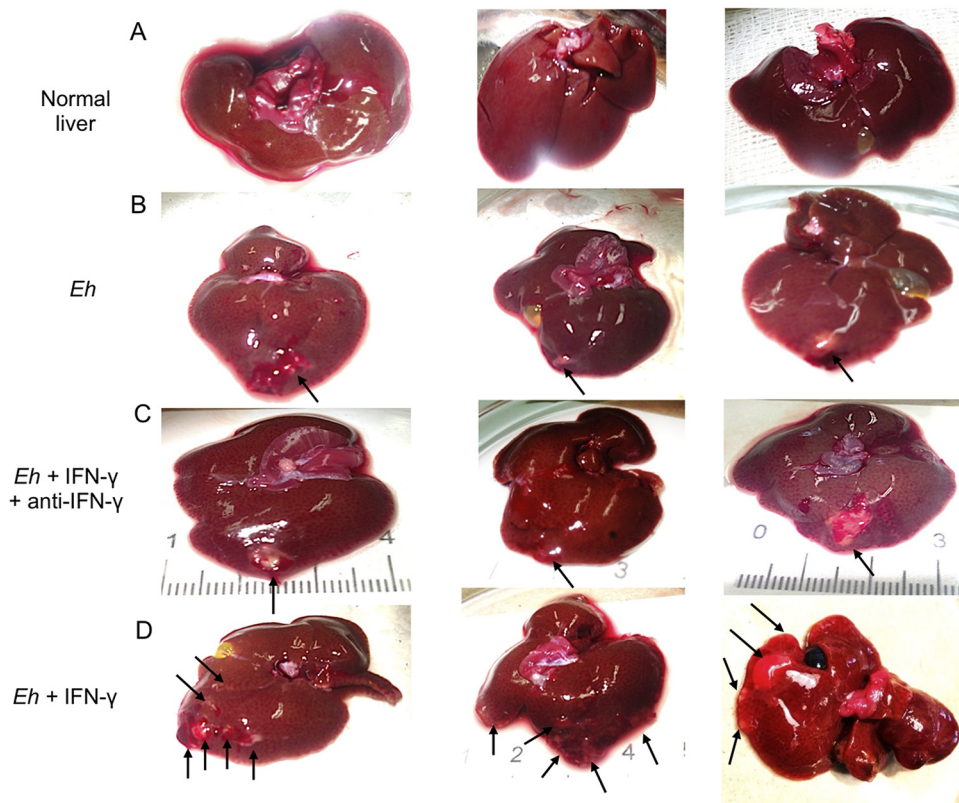


**FIG 10** Amebic liver abscesses (ALA) 4 days postinoculation. Macroscopic development of ALA in male hamsters inoculated with *E. histolytica* trophozoites with or without stimulation with IFN- $\gamma$  for 20 min. (A) Control uninfected livers of hamsters. (B) Single lesions (arrows) are seen in the liver lobes inoculated with *E. histolytica*. (C) The lesions (arrows) in the livers of hamsters treated with IFN- $\gamma$  and anti-IFN- $\gamma$  antibody appear similar to the ALA formed by control *E. histolytica* trophozoites, shown in panel B. (D) Morphology of ALA when *E. histolytica* trophozoites were pretreated with IFN- $\gamma$ , demonstrating several granulomas distributed in the left and right lobes of the livers (arrows).

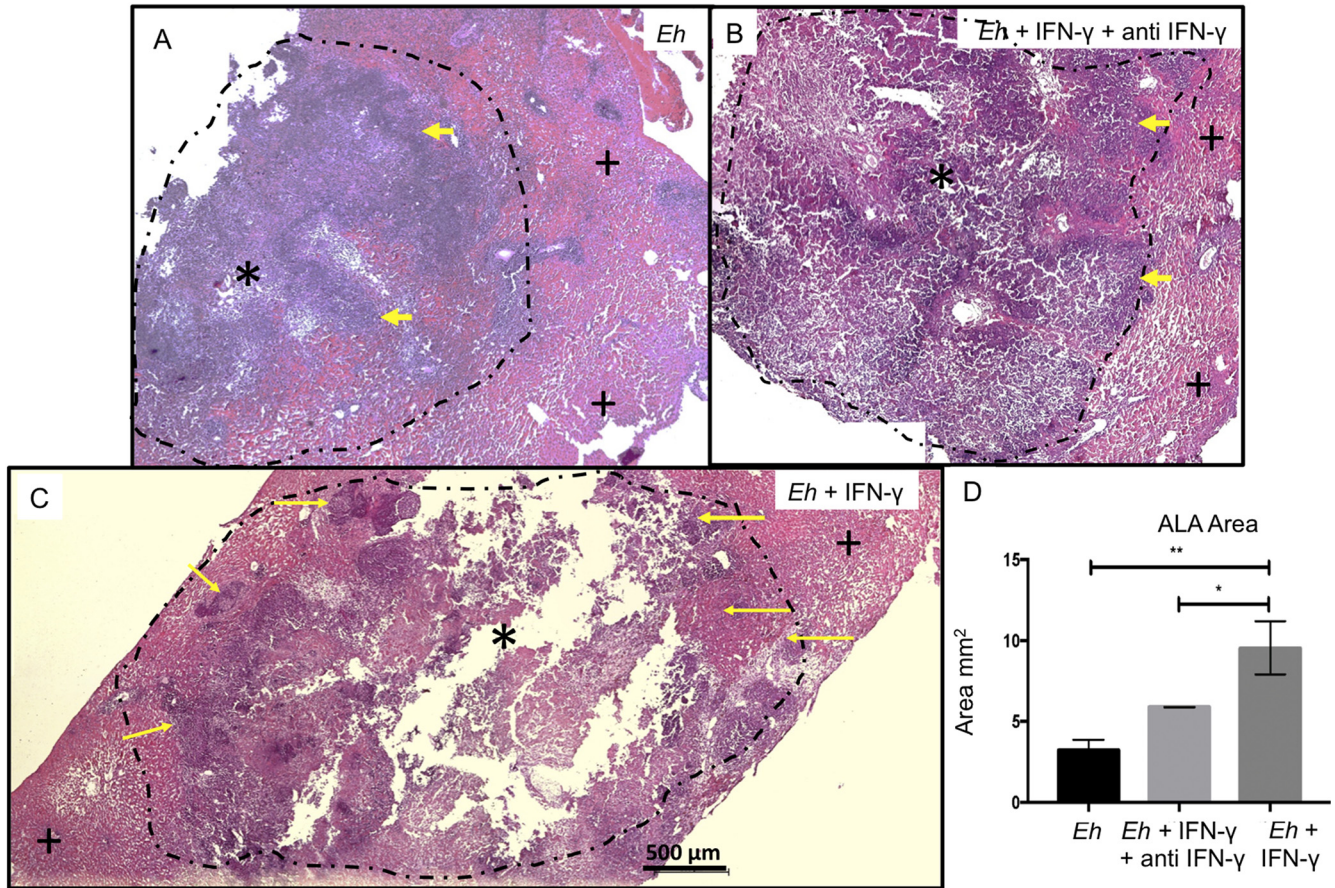


**FIG 11** (A) Normal development of ALA. Necrotic tissue is seen in the center of the lesion (\*), and the edges show areas of inflammatory infiltrate (arrowheads) that are in contact with healthy areas of the liver (+). (B) ALA formed by *E. histolytica* trophozoites in the presence of IFN- $\gamma$ -anti-IFN antibody complex: the distribution of necrotic area and inflammatory infiltrates is similar to those of ALA induced by *E. histolytica* trophozoites. (C) ALA formed by *E. histolytica* trophozoites preincubated with IFN- $\gamma$  (100 ng/ml). Note increased ALA development with multiple zones of new inflammatory infiltrate (yellow arrows) at the periphery of the lesions. The black dashed-line circles indicate the zones of ALA development. Hematoxylin-and-eosin staining was used. (D) Quantification of ALA development. One-way ANOVA and Tukey's *post hoc* test were used. \*,  $P < 0.05$ ; \*\*,  $P < 0.01$ .

intestinal amebiasis in children (37). In tissues, *E. histolytica* evades host immune cells by phagocytosis or apoptosis (38), by trogocytosis (39), or by inhibiting IFN- $\gamma$  production with prostaglandin E<sub>2</sub> (PGE<sub>2</sub>) from the cyclooxygenase (Cox)-like enzyme (5, 40, 41). By Western blot analysis, using an anti-human IFN- $\gamma$ R1 antibody, we detected the presence of an *E. histolytica* protein of ~200 kDa in membrane fractions. This suggests that IFN- $\gamma$  produced at the site of lesions is likely to bind the 200-kDa *E. histolytica* protein. By sequencing and *in silico* analysis, the 200-kDa protein showed similarity to a putative tyrosine kinase protein, with 50% homology in amino acid and physico-chemical characteristics to the motif that binds human IFN- $\gamma$  receptor.

The binding between IFN- $\gamma$  and human immune cells is well characterized (42) for functional activity, including the release of various proinflammatory mediators critical in inflammation. Our finding of an IFN- $\gamma$  receptor-like protein on the *E. histolytica* membrane with homology to the binding motif of human IFN- $\gamma$  receptor is remarkable. Consistent with an IFN- $\gamma$  receptor-like protein, exposure of *E. histolytica* trophozoites to IFN- $\gamma$  increased their phagocytosis of erythrocytes by 15 times in a STAT1-dependent manner and upregulated several virulence genes that enhance adherence to host cells and proteases that degrade extracellular substrates. Equally important was the finding of chemotaxis of *E. histolytica* trophozoites toward IFN- $\gamma$ , which demonstrates that *E. histolytica* can sense proinflammatory cytokines in lesions. Similar findings have been described for *E. histolytica* sensing IL-8 and TNF- $\alpha$  (21, 22). IFN- $\gamma$  also significantly increased *E. histolytica*'s cytotoxicity against Caco2 and HepG2 cells. This effect may be



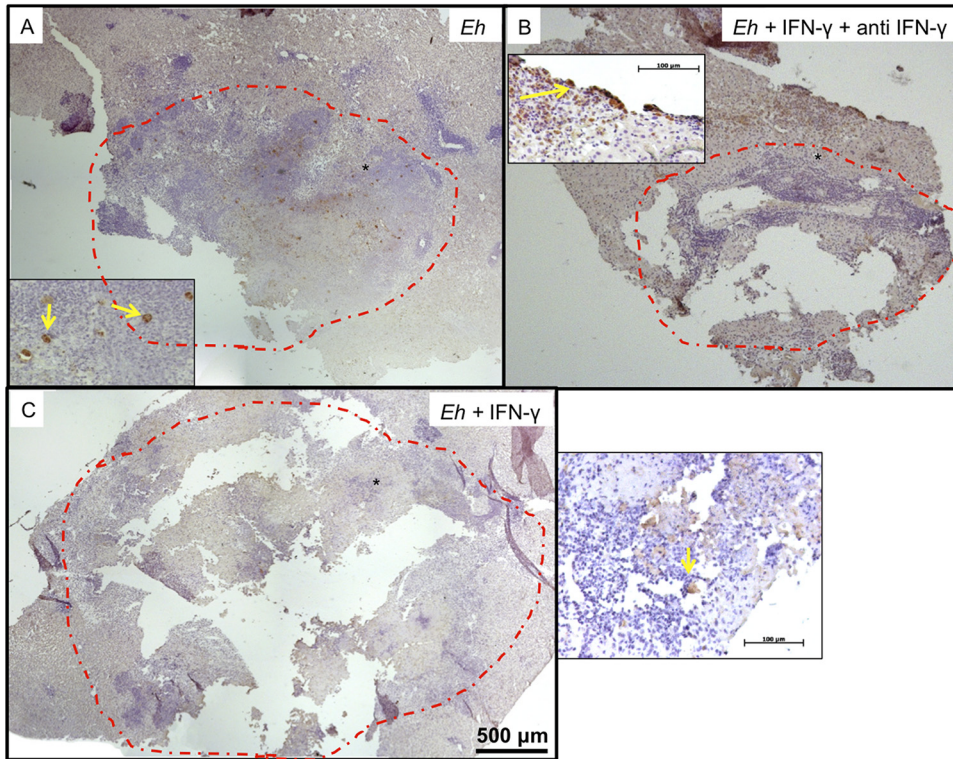


**FIG 12** Immunohistochemical detection of *E. histolytica* trophozoites in hamster ALA. (A) ALA formed by control *E. histolytica* trophozoites. (B) ALA formed by *E. histolytica* trophozoites treated with IFN- $\gamma$ -anti-IFN- $\gamma$  complex. (C) ALA formed by *E. histolytica* trophozoites treated with IFN- $\gamma$ . The red dashed-line circles indicate the zones of ALA development. In insets, the yellow arrows show *E. histolytica* trophozoites in liver tissues. The asterisk indicates the location zone of *E. histolytica* trophozoites.

related to increased expression of *Eh*CPs and upregulation of the Gal/GalNAc lectin to allow the parasite to disrupt innate mucosal barriers (29, 30, 43). ALA formation in hamster livers showed that *E. histolytica* trophozoites exposed to IFN- $\gamma$  became more virulent, resulting in greater lesion sizes with multiple granulomas and metastatic foci to other liver lobes. Increased ALA formation due to preexposure of *E. histolytica* trophozoites to IFN- $\gamma$  is a novel observation and perhaps is a strategy used by *E. histolytica* to bind to and deplete IFN- $\gamma$  in ALA lesions. This is especially important as IFN- $\gamma$  can activate newly recruited inflammatory macrophages and neutrophils to sites of infection, which is detrimental to *E. histolytica*. Thus, the ability of *E. histolytica* to bind and increase cytotoxicity toward inflammatory cells represents a strong immune evasion strategy by the parasite. In summary, our findings show that *E. histolytica* expresses a functional protein similar to human IFN- $\gamma$ R1 that functions by upregulating several key virulence factors that enhance erythrophagocytosis and cytotoxicity of epithelial cells and are critical in disease pathogenesis and immune evasion.

## MATERIALS AND METHODS

***E. histolytica* culture.** *E. histolytica* HM-1:IMSS trophozoites were grown axenically in TYI-S-33 medium containing 10% bovine serum and supplemented with penicillin (100 U/ml), streptomycin (100  $\mu$ g/ml), and 10% heat-inactivated adult bovine serum, as previously described (43). To maintain virulence, trophozoites were regularly passed through golden hamster (*Mesocricetus auratus*) livers as described previously (44). Trophozoites were harvested in the logarithmic phase of growth (48 to 72 h) by cooling the culture tubes on ice and centrifuging the cell suspensions at  $300 \times g$  for 15 min. Recovered *E. histolytica* trophozoites were suspended in culture medium without serum, pH 7.2, for the assays.

**Immunofluorescence detection of IFN- $\gamma$  fixed on *E. histolytica* trophozoites.** For double immunofluorescence assays, *E. histolytica* trophozoites ( $2 \times 10^5$ ) were cultured in coverslips in a petri dish with TYI-S-33 medium (Trypticase, yeast extract, iron serum) for 15 min at 37°C. Coverslips were washed three times with phosphate-buffered saline (PBS), medium supplemented with IFN- $\gamma$  (100 ng/ml; Peprotech,

Rocky Hill, NJ, USA) was added, and the trophozoites were incubated for 20, 60, or 180 min at 37°C. Coverslips were washed three times with PBS, and the trophozoites were fixed with 4% paraformaldehyde for 20 min and blocked with 10% fetal bovine serum in PBS for 1 h at 37°C. The preparations were incubated overnight at 4°C with primary antibodies anti-IFN- $\gamma$  antibody (1:100) (catalog number 500-P32; Peprotech) and anti-IFN- $\gamma$ R1 antibody (1:100) (catalog number MA5-16583; Thermo Fisher Scientific). After three washes with PBS, secondary antibodies (1:1,000) Alexa Fluor 594-conjugated goat anti-mouse IgG(H+L) (catalog number A11005; Thermo Fisher Scientific) and Alexa Fluor 488-conjugated goat anti-rabbit IgG(H+L) (catalog number A11008; Thermo Fisher Scientific) were added and the preparations were incubated overnight at 4°C. Nuclei were stained with Hoechst stain (1  $\mu$ g/ml; Thermo Fisher Scientific) in PBS for 10 min at room temperature. Coverslips were mounted with Vectashield (Vector Laboratories, Burlingame, CA, USA) and analyzed in an LMS700 microscope (Zeiss). Images were processed with ZEN 2009 Light Edition software (Zeiss). To quantify colocalization, 1- $\mu$ m z-stacks of entire cells or an area around the plasma membrane were analyzed according to the Costes methodology, which includes the elimination of autofluorescence with the Coloc2 plugin of Fiji software (ImageJ). Graphing was done with GraphPad Prism 7 software (45).

**Western blot analysis for detecting IFN- $\gamma$ R1 on *E. histolytica* trophozoite membranes.** *E. histolytica* trophozoites were cultured in the presence or absence of 100 ng/ml of recombinant IFN- $\gamma$  (Peprotech, Rocky Hill, NJ, USA) for 20 min at 37°C. After incubation, trophozoites were washed with PBS. For protein extraction, approximately  $1 \times 10^6$  cells were resuspended in 1 ml of lysis buffer with protease inhibitors (50 mM Tris-HCl, pH 6.8, 5 mM *N*-ethylmaleimide, 3 mM iodoacetamide, 1 mM phenylmethanesulfonyl fluoride, and 3 mM tosyl-L-lysine chloromethyl ketone). All inhibitors were purchased from Sigma-Aldrich. The cells were homogenized with  $-70^{\circ}\text{C}/37^{\circ}\text{C}$  incubation cycles. The lysates were centrifuged at  $40,000 \times g$  for 1 h at 4°C. The supernatant and pellet correspond to the cytosolic and membrane fraction, respectively. Positive-control human leukocyte total lysates were collected as well. Then, the pellets were suspended in 200  $\mu$ l lysis buffer and 2.5% Triton X-100. Protein quantification was performed with the Bradford method (46). For Western blotting, 50  $\mu$ g of each protein extract was separated in a 10% SDS-PAGE gel, and proteins were transferred to polyvinylidene difluoride (PVDF) membranes (Bio-Rad, Hercules, CA, USA). The membranes were blocked with Tris-buffered saline (TBS) and 5% skimmed milk for 1 h at room temperature. For immunodetection, the membranes were incubated for 24 h at 4°C with the primary antibody, a mouse anti-IFN- $\gamma$ R1 monoclonal antibody (1:1000; Thermo Fisher Scientific, Waltham, MA, USA). Blots were incubated with goat anti-mouse IgG conjugated with Alexa Fluor 594 (1:5,000; Millipore, Burlington, MA, USA). After the incubation, the membranes were washed with TBST (Tris-buffered saline–0.05% Tween 20) and blots were developed with Clarity Western ECL substrate (Bio-Rad, Hercules CA, USA) for chemiluminescence imaging.

**Isolation of total RNA and qPCR.** Total RNA was isolated from  $1 \times 10^6$  *E. histolytica* trophozoites incubated or not with IFN- $\gamma$  for 0, 10, 20, 30, and 60 min, using the SV total RNA isolation system (Promega, Madison, WI, USA) according to the manufacturer's protocol. Reverse transcription was performed with 50 ng of total RNA from *E. histolytica* trophozoites using the GoScript reverse transcription system (catalog number a5001; Promega), followed by real-time quantitative PCR (qPCR) analysis using qPCR GreenMaster with UNG, clear (Jena Bioscience, Jena, Germany) in a StepOne machine (Applied Biosystems) with the following program: 50°C for 2 min, 95°C for 3 min, and 40 cycles of 95°C for 30 s and 60°C for 30 s. Oligonucleotides were designed to target genes encoding *E. histolytica* cysteine proteases 1, 2, 4, and 5, amebapore, Cox-1, Gal/GalNAc lectin, and peroxiredoxin (Table S1 in the supplemental material). Relative expression levels were normalized against the expression of the respective *E. histolytica* genes from cells cultured without stimuli as an internal control, and differences were determined by employing the  $\Delta\Delta C_T$  relative method. The rRNA gene was used as the housekeeping gene, using the StepOne machine (Applied biosystem).

**Erythrophagocytosis.** *E. histolytica* trophozoites were cultured in glass tubes under axenic conditions. Trophozoites ( $2 \times 10^6$ ) were harvested by chilling the culture tubes at 4°C in a water-ice bath for 10 min and then centrifuging them at  $300 \times g$  for 5 min and washing with sterile Dulbecco's PBS (DPBS) (catalog number D8537; Sigma-Aldrich). To abrogate signaling via IFN- $\gamma$ R1, trophozoites were pretreated with the STAT1 inhibitor fludarabine at 50  $\mu$ M (catalog number Sc-204755; Santa Cruz) for 30 min before exposure to IFN- $\gamma$  (100 ng/ml) for 20 min. Following incubation, trophozoites were washed twice with DPBS before the assay. Fresh human erythrocytes in DPBS solution were stained with PKH26 (catalog number MINI26; Sigma-Aldrich), counted, and used at a 1:100 (trophozoites/erythrocytes) ratio. To establish the interaction, erythrocytes were added, and the interaction was carried out for 20 min at 37°C in DPBS, after which they were washed twice with DPBS. Lysis buffer (red blood cell [RBC] lysing buffer) (catalog number R7757; Sigma-Aldrich) was added for 1 min at room temperature. Fetal bovine serum (FBS; 0.5 ml) (catalog number 10437-028; Gibco) was added for 1 min at room temperature, and the cells were washed once with DPBS. The cells were fixed with 4% paraformaldehyde for 20 min at room temperature and washed with DPBS, removing as much liquid as possible from the sample. To each tube was added a drop of FluorSave reagent (catalog number 345789; Calbiochem), and the contents were mixed carefully, placed on a clean slide, and stored in the dark at 4°C for at least 24 h before being observed under a microscope.

**Immunoprecipitation.** *E. histolytica* trophozoites were cultured in glass tubes under axenic conditions. Trophozoites were harvested by chilling the culture tubes at 4°C in a water-ice bath for 10 min, and then they were centrifuged at  $300 \times g$  for 5 min and washed with sterile DPBS (Sigma-Aldrich). Trophozoites were treated with fludarabine (50  $\mu$ M) at 37°C for 30 min and then stimulated with IFN- $\gamma$  (100 ng/ml) at 37°C for 20 min. Lysates were prepared from trophozoites by using a modified protocol (47). *E. histolytica* trophozoites were washed twice in cold PBS and suspended in radioimmunoprecipi-

tation assay (RIPA) buffer containing protease inhibitor cocktail (Sigma), phenylmethylsulfonyl fluoride (PMSF), sodium fluoride, and sodium orthovanadate. Lysates were centrifuged at  $10,000 \times g$  for 10 min. Immunoprecipitation was carried out using 200  $\mu\text{g}$  of protein, and the primary antibody (anti-phospho-Tyr antibody, 1.5  $\mu\text{g}$ ; BD transduction laboratories) was incubated with the supernatant for 8 h at 4°C, followed by 12 h at 4°C with protein A/G plus-agarose (Santa Cruz Biotechnology). Samples were run on 7.5% SDS-PAGE gels and probed with antibodies as follows: anti-STAT1 antibody (Santa Cruz) and anti-phospho-STAT1 antibody (Abcam).

**Chemotaxis.** Chemotaxis of *E. histolytica* trophozoites toward IFN- $\gamma$  was monitored in Transwell migration chambers (catalog number 3464; Corning) as previously reported (48). The chemoattractant gradients were generated by placing 600  $\mu\text{l}$  of culture medium without serum and containing 100 ng/ml of IFN- $\gamma$  in the lower chamber of the migration units and 30,000 *E. histolytica* trophozoites on the filter of the upper Transwell chamber. Cells were maintained under 0.05% CO<sub>2</sub> conditions at 37°C for 30 min. Cells that migrated toward IFN- $\gamma$  and reached the lower chamber were recovered, stained with crystal violet, and quantified in an inverted microscope. To inhibit chemotaxis toward IFN- $\gamma$ , trophozoites were treated with cytochalasin D, which depolymerizes actin/myosin filaments, as previously described (21). A coverslip chemotaxis gradient assay was used to visualize individual migrating *E. histolytica* trophozoites; for this, 180  $\mu\text{l}$  of serum-depleted medium containing 100 ng/ml of IFN- $\gamma$  was injected into a 0.75% agarose strip placed along one edge of each coverslip. On the opposite edge, trophozoites were placed along a narrow band and allowed to attach to the glass for 20 min. Chemotaxis of trophozoites toward IFN- $\gamma$  (100 ng) was visualized using phase-contrast video microscopy. Video registers were made with a Carl Zeiss Axiovert 40CFL inverted microscope and the digital camera used in the immunofluorescence assays. Time-lapse videos were generated from 114 spaced frames, with 2 s between each frame acquired for 4-min real-time registers. Each video was processed with AxioVision 40V 4.6.3.0 software. To register random motility of trophozoites in the absence of IFN- $\gamma$ , agarose strips not containing IFN- $\gamma$  and only injected with serum-free culture medium were placed on one edge of coverslips, and migration was recorded as described above. The data analysis was performed using ImageJ 1.51n (<http://imagej.nih.gov/ij>).

**Cytotoxicity assay.** Human adenocarcinoma Caco-2 cells and human liver cancer HepG2 cells from ATCC were grown to confluent monolayers in Dulbecco's modified Eagle's medium (DMEM) (catalog number 11995-040; Thermo Fisher) with 10% serum, penicillin, and streptomycin for 3 days (modified from the procedures in references 49 and 50). Cells grown in 24-well plates to 80 to 90% confluence were washed twice with DPBS, and 500  $\mu\text{l}$  of DMEM medium was added per well. *E. histolytica* trophozoites ( $1 \times 10^5$  per well) were treated or not with the STAT1 inhibitor fludarabine (50  $\mu\text{M}$ ) (catalog number Sc-204755; Santa Cruz) for 30 min prior to IFN- $\gamma$  (100 ng/ml) stimulation for 20 min. For the interaction, trophozoites were added to each well for 1 h. After incubation, the cells were placed on ice, washed with DPBS, and fixed with 2.5% paraformaldehyde for 10 min. The monolayer was stained with 0.1% methylene blue in 0.1 M borate buffer (pH 8) for 10 min at room temperature. The plates were washed with 0.1 M borate buffer twice to remove excess stain. Finally, 1 ml of 1 N HCl was added to each well for 30 min at 37°C to extract the stain, and the absorbance read on a spectrometer at 655 nm (optical density at 655 nm [OD<sub>655</sub>]). The percentage of monolayer destruction was calculated as follows:  $[\text{OD}_{655}(\text{control wells}) - \text{OD}_{655}(\text{experimental wells}) / \text{OD}_{655}(\text{control wells})] \times 100$ .

**Animals.** Male golden hamsters (*Mesocricetus auratus*) weighing 140 to 160 g were used in this study. The animals were maintained on standard diet with free access to drinking water. All animals received humane care according to the guidelines of the Committee on Bioethics in the animal facilities of the Autonomous University of Aguascalientes, Aguascalientes, Mexico, which are based on the guidelines for animal research published by the National Institutes of Health (51).

**Experimental hepatic amebiasis.** *E. histolytica* trophozoites ( $5 \times 10^5$ ) were incubated in the presence or absence of 100 ng/ml of recombinant IFN- $\gamma$  (Peprotech, Rocky Hill, NJ, USA) for 20 min. After incubation, trophozoites were washed with PBS and inoculated into the left liver lobe of hamsters in 100  $\mu\text{l}$  of culture medium as previously described (44, 52). After 4 days, the animals were anaesthetized with sodium pentobarbital (50 mg/kg of body weight intraperitoneally), the liver was excised for macroscopic evaluation, and several specimens that included ALA were taken, fixed in 4% paraformaldehyde, and processed for histological analysis.

**H&E staining.** To visualize ALA development, we performed hematoxylin and eosin (H&E) staining as described in the *Manual of Histologic Staining Methods of the Armed Forces* (53). The sample tissues were analyzed to determine the percentages of necrotic and inflammatory areas using ImageJ software.

**Immunohistochemistry.** To visualize the presence of *E. histolytica* trophozoites in liver tissue, sections were subjected to immunohistochemistry as described previously (53). For *E. histolytica* immunodetection, the samples were incubated with the primary antibody rabbit anti-*E. histolytica* antibody, raised in our laboratory, diluted 1:400 at 4°C. The secondary antibody, goat anti-rabbit IgG, was diluted 1:500 (Sigma-Aldrich) and incubated for 2 h at room temperature. Slides were washed with PBS-Tween 20 for 10 min, and peroxidase activity was developed with diaminobenzidine (DAB) (Pierce Biotechnology, Inc., Rockford, IL, USA) for 5 min.

**Statistical analysis.** Statistical analyses were performed using GraphPad Prism version 5.01 (GraphPad Software, San Diego, CA, USA). Student's *t* test and one-way analysis of variance (ANOVA) with Tukey's *post hoc* test were used. Differences between groups were assessed as significant at a *P* value of <0.05. Experimental results are represented in the figures as the mean values from three independent experiments  $\pm$  standard deviations (SD).



## SUPPLEMENTAL MATERIAL

Supplemental material for this article may be found at <https://doi.org/10.1128/IAI.00540-19>.

**SUPPLEMENTAL FILE 1**, PDF file, 0.04 MB.

**SUPPLEMENTAL FILE 2**, MP4 file, 2.2 MB.

**SUPPLEMENTAL FILE 3**, MP4 file, 3.4 MB.

## ACKNOWLEDGMENTS

We thank UAA for the PIBB16-2 grant to Javier Ventura-Juárez and acknowledge a discovery grant (grant number RGPIN-2019-04136) from the Natural Sciences and Engineering Research Council of Canada awarded to Kris Chadee, CONACYT doctoral fellowships to Julieta Pulido-Ortega (grant number 290934) and Aralia Leon-Coria (grant number 314101), postdoctoral support given to Liseth Rubí Aldaba-Muruato (grant number 176507), and a CONACYT grant to Javier Ventura-Juárez (grant number 286184).

We thank Manuel Enrique Avila-Blanco for image analysis.

We declare no conflict of interest.

## REFERENCES

- Bruckner DA. 1992. Amebiasis. *Clin Microbiol Rev* 5:356–369. <https://doi.org/10.1128/cmr.5.4.356>.
- Chávez-Munguía B, Talamás-Rohana P, Castañón G, Salazar-Villatoro L, Hernández-Ramírez V, Martínez-Palomo A. 2012. Differences in cap formation between invasive *Entamoeba histolytica* and non-invasive *Entamoeba dispar*. *Parasitol Res* 111:215–221. <https://doi.org/10.1007/s00436-012-2820-2>.
- García-Nieto RM, Rico-Mata R, Arias-Negrete S, Avila EE. 2008. Degradation of human secretory IgA1 and IgA2 by *Entamoeba histolytica* surface-associated proteolytic activity. *Parasitol Int* 57:417–423. <https://doi.org/10.1016/j.parint.2008.04.013>.
- Talamás-Rohana P, Schlie-Guzmán MA, Hernández-Ramírez VI, Rosales-Encina JL. 1995. T-cell suppression and selective in vivo activation of TH2 subpopulation by the *Entamoeba histolytica* 220-kilodalton lectin. *Infect Immun* 63:3953–3958.
- Wang W, Chadee K. 1995. *Entamoeba histolytica* suppresses gamma interferon-induced macrophage class II major histocompatibility complex Ia molecule and I-A beta mRNA expression by a prostaglandin E2-dependent mechanism. *Infect Immun* 63:1089–1094.
- Sabeti PC, Schaffner SF, Fry B, Lohmueller J, Varilly P, Shamovsky O, Palma A, Mikkelsen TS, Altshuler D, Lander ES. 2006. Positive natural selection in the human lineage. *Science* 312:1614–1620. <https://doi.org/10.1126/science.1124309>.
- Woolhouse MEJ, Webster JP, Domingo E, Charlesworth B, Levin BR. 2002. Biological and biomedical implications of the co-evolution of pathogens and their hosts. *Nat Genet* 32:569–577. <https://doi.org/10.1038/ng1202-569>.
- Moncada D, Keller K, Chadee K. 2003. *Entamoeba histolytica* cysteine proteinases disrupt the polymeric structure of colonic mucin and alter its protective function. *Infect Immun* 71:838–844. <https://doi.org/10.1128/iai.71.2.838-844.2003>.
- Dey I, Chadee K. 2008. Prostaglandin E2 produced by *Entamoeba histolytica* binds to EP4 receptors and stimulates interleukin-8 production in human colonic cells. *Infect Immun* 76:5158–5163. <https://doi.org/10.1128/IAI.00645-08>.
- Gilchrist CA, Petri WA. 1999. Virulence factors of *Entamoeba histolytica*. *Curr Opin Microbiol* 2:433–437. [https://doi.org/10.1016/S1369-5274\(99\)80076-9](https://doi.org/10.1016/S1369-5274(99)80076-9).
- Chadee K, Petri WA, Innes DJ, Ravdin JI. 1987. Rat and human colonic mucins bind to and inhibit adherence lectin of *Entamoeba histolytica*. *J Clin Invest* 80:1245–1254. <https://doi.org/10.1172/JCI113199>.
- Lidell ME, Moncada DM, Chadee K, Hansson GC. 2006. *Entamoeba histolytica* cysteine proteases cleave the MUC2 mucin in its C-terminal domain and dissolve the protective colonic mucus gel. *Proc Natl Acad Sci U S A* 103:9298–9303. <https://doi.org/10.1073/pnas.0600623103>.
- Kelsall BL, Ravdin JI. 1993. Degradation of human IgA by *Entamoeba histolytica*. *J Infect Dis* 168:1319–1322. <https://doi.org/10.1093/infdis/168.5.1319>.
- Gilmartin AA, Ralston KS, Petri WA. 2017. Inhibition of amebic lysosomal acidification blocks amebic trophocytosis and cell killing. *mBio* 8:e01187-17. <https://doi.org/10.1128/mBio.01187-17>.
- Calderón J, de Lourdes Muñoz M, Acosta HM. 1980. Surface redistribution and release of antibody-induced caps in entamoebae. *J Exp Med* 151:184–193. <https://doi.org/10.1084/jem.151.1.184>.
- Bruchhaus I, Richter S, Tannich E. 1997. Removal of hydrogen peroxide by the 29 kDa protein of *Entamoeba histolytica*. *Biochem J* 326:785–789. <https://doi.org/10.1042/bj3260785>.
- Davis PH, Zhang Z, Chen M, Zhang X, Chakraborty S, Stanley SL. 2006. Identification of a family of BspA like surface proteins of *Entamoeba histolytica* with novel leucine rich repeats. *Mol Biochem Parasitol* 145: 111–116. <https://doi.org/10.1016/j.molbiopara.2005.08.017>.
- Flores-Romo L, Tsutsumi V, Estrada-García T, Shibayama M, Aubry JP, Bacon KB, Martínez-Palomo A. 1994. CD59 (protectin) molecule, resistance to complement, and virulence of *Entamoeba histolytica*. *Trans R Soc Trop Med Hyg* 88:116–117. [https://doi.org/10.1016/0035-9203\(94\)90530-4](https://doi.org/10.1016/0035-9203(94)90530-4).
- Goplen M, Lejeune M, Cornick S, Moreau F, Chadee K. 2013. *Entamoeba histolytica* contains an occludin-like protein that can alter colonic epithelial barrier function. *PLoS One* 8:e73339. <https://doi.org/10.1371/journal.pone.0073339>.
- Mancilla-Herrera I, Méndez-Tenorio A, Wong-Baeza I, Jiménez-Urbe AP, Alcántara-Hernández M, Ocádiz-Ruiz R, Moreno-Eutimio MA, Arriaga-Pizano LA, López-Macías C, González-y-Merchand J, Isibasi A. 2012. A Toll/IL-1R/resistance domain-containing thioredoxin regulates phagocytosis in *Entamoeba histolytica*. *Parasit Vectors* 5:224. <https://doi.org/10.1186/1756-3305-5-224>.
- Díaz-Valencia JD, Pérez-Yépez EA, Ayala-Sumano JT, Franco E, Meza I. 2015. A surface membrane protein of *Entamoeba histolytica* functions as a receptor for human chemokine IL-8: its role in the attraction of trophozoites to inflammation sites. *Int J Parasitol* 45:915–923. <https://doi.org/10.1016/j.ijpara.2015.07.007>.
- Blazquez S, Zimmer C, Guigon G, Olivo-Marin J-C, Guillén N, Labruyère E. 2006. Human tumor necrosis factor is a chemoattractant for the parasite *Entamoeba histolytica*. *Infect Immun* 74:1407–1411. <https://doi.org/10.1128/IAI.74.2.1407-1411.2006>.
- Castellanos C, Ramos C, Ortiz-Ortiz L. 1989. Effects of gamma interferon on syntheses of DNA and proteins by *Entamoeba histolytica*. *Infect Immun* 57:2771–2775.
- Sierra-Puente RE, Campos-Rodríguez R, Jarillo-Luna RA, Muñoz-Fernández L, Rodríguez MG, Muñoz-Ortega MH, Ventura-Juárez J. 2009. Expression of immune modulator cytokines in human fulminant amoebic colitis. *Parasite Immunol* 31:384–391. <https://doi.org/10.1111/j.1365-3024.2009.01118.x>.
- Talamás-Lara D, Chávez-Munguía B, González-Robles A, Talamás-Rohana P, Salazar-Villatoro L, Durán-Díaz Á, Martínez-Palomo A. 2014. Erythrophagocytosis in *Entamoeba histolytica* and *Entamoeba dispar*: a com-

- parative study. *BioMed Res Int* 2014;1–10. <https://doi.org/10.1155/2014/626259>.
26. Bailey GB, Leitch GJ, Day DB. 1985. Chemotaxis by *Entamoeba histolytica*. *J Protozool* 32:341–346. <https://doi.org/10.1111/j.1550-7408.1985.tb03063.x>.
  27. Yu Y, Chadee K. 1997. *Entamoeba histolytica* stimulates interleukin 8 from human colonic epithelial cells without parasite-enterocyte contact. *Gastroenterology* 112:1536–1547. [https://doi.org/10.1016/s0016-5085\(97\)70035-0](https://doi.org/10.1016/s0016-5085(97)70035-0).
  28. Katz U, Anki S, Stolarsky T, Nuchamowitz Y, Mirelman D. 2002. *Entamoeba histolytica* expressing a dominant negative N-truncated light subunit of its gal-lectin are less virulent. *Mol Biol Cell* 13:4256–4265. <https://doi.org/10.1091/mbc.e02-06-0344>.
  29. Begum S, Quach J, Chadee K. 2015. Immune evasion mechanisms of *Entamoeba histolytica*: progression to disease. *Front Microbiol* 6:1394. <https://doi.org/10.3389/fmicb.2015.01394>.
  30. Nakada-Tsukui K, Nozaki T. 2016. Immune response of amebiasis and immune evasion by *Entamoeba histolytica*. *Front Immunol* 7:175. <https://doi.org/10.3389/fimmu.2016.00175>.
  31. Olivos-García A, Saavedra E, Ramos-Martínez E, Nequiz M, Pérez-Tamayo R. 2009. Molecular nature of virulence in *Entamoeba histolytica*. *Infect Genet Evol* 9:1033–1037. <https://doi.org/10.1016/j.meegid.2009.04.005>.
  32. Rico G, Leandro E, Rojas S, Giménez JA, Kretschmer RR. 2003. The monocyte locomotion inhibitory factor produced by *Entamoeba histolytica* inhibits induced nitric oxide production in human leukocytes. *Parasitol Res* 90:264–267. <https://doi.org/10.1007/s00436-002-0780-7>.
  33. del Villalobos-Gómez FR, García-Lorenzana M, Escobedo G, Talamás-Rohana P, Salinas-Gutiérrez R, Hernández-Ramírez V-I, Sánchez-Alemán E, del Campos-Esparza MR, Muñoz-Ortega MH, Ventura-Juárez J. 2018. *Entamoeba histolytica* L220 induces the in vitro activation of macrophages and neutrophils and is modulated by neurotransmitters. *Acta Parasitol* 63:270–279. <https://doi.org/10.1515/ap-2018-0031>.
  34. Ngobeni R, Abhyankar MM, Jiang NM, Farr LA, Samie A, Haque R, Moonah SN. 2017. *Entamoeba histolytica*-encoded homolog of macrophage migration inhibitory factor contributes to mucosal inflammation during amebic colitis. *J Infect Dis* 215:1294–1302. <https://doi.org/10.1093/infdis/jix076>.
  35. Guo X, Stroup SE, Houpt ER. 2008. Persistence of *Entamoeba histolytica* infection in CBA mice owes to intestinal IL-4 production and inhibition of protective IFN- $\gamma$ . *Mucosal Immunol* 1:139–146. <https://doi.org/10.1038/mi.2007.18>.
  36. Salata RA, Pearson RD, Ravdin JI. 1985. Interaction of human leukocytes and *Entamoeba histolytica*. Killing of virulent amebae by the activated macrophage. *J Clin Invest* 76:491–499. <https://doi.org/10.1172/JCI111998>.
  37. Haque R, Mondal D, Shu J, Roy S, Kabir M, Davis AN, Duggal P, Petri WA, Jr. 2007. Correlation of interferon- $\gamma$  production by peripheral blood mononuclear cells with childhood malnutrition and susceptibility to amebiasis. *Am J Trop Med Hyg* 76:340–344. <https://doi.org/10.4269/ajtmh.2007.76.340>.
  38. Huston CD, Boettner DR, Miller-Sims V, Petri WA, Jr. 2003. Apoptotic killing and phagocytosis of host cells by the parasite *Entamoeba histolytica*. *Infect Immun* 71:964–972. <https://doi.org/10.1128/IAI.71.2.964-972.2003>.
  39. Ralston KS. 2015. Taking a bite: amoebic trophocytosis in *Entamoeba histolytica* and beyond. *Curr Opin Microbiol* 28:26–35. <https://doi.org/10.1016/j.mib.2015.07.009>.
  40. Dey I, Keller K, Belley A, Chadee K. 2003. Identification and characterization of a cyclooxygenase-like enzyme from *Entamoeba histolytica*. *Proc Natl Acad Sci U S A* 100:13561–13566. <https://doi.org/10.1073/pnas.1835863100>.
  41. Shahi P, Moreau F, Chadee K. 2019. *Entamoeba histolytica* cyclooxygenase-like protein regulates cysteine protease expression and virulence. *Front Cell Infect Microbiol* 8:447. <https://doi.org/10.3389/fcimb.2018.00447>.
  42. Bach EA, Aguet M, Schreiber RD. 1997. The IFN- $\gamma$  receptor: a paradigm for cytokine receptor signaling. *Annu Rev Immunol* 15:563–591. <https://doi.org/10.1146/annurev.immunol.15.1.563>.
  43. Diamond LS, Harlow DR, Cunnick CC. 1978. A new medium for the axenic cultivation of *Entamoeba histolytica* and other *Entamoeba*. *Trans R Soc Trop Med Hyg* 72:431–432. [https://doi.org/10.1016/0035-9203\(78\)90144-x](https://doi.org/10.1016/0035-9203(78)90144-x).
  44. Tsutsumi V, Mena-Lopez R, Anaya-Velazquez F, Martinez-Palomo A. 1984. Cellular bases of experimental amebic liver abscess formation. *Am J Pathol* 117:81–91.
  45. Schneider CA, Rasband WS, Eliceiri KW. 2012. NIH Image to ImageJ: 25 years of image analysis. *Nat Methods* 9:671–675. <https://doi.org/10.1038/nmeth.2089>.
  46. Bradford MM. 1976. A rapid and sensitive method for the quantitation of microgram quantities of protein utilizing the principle of protein-dye binding. *Anal Biochem* 72:248–254. <https://doi.org/10.1006/abio.1976.9999>.
  47. Cruz-Vera J, Clara L, Hernández-Kelly R, Alfredo-Méndez J, Pérez-Salazar E, Ortega A. 2003. Collagen-induced STAT family members activation in *Entamoeba histolytica* trophozoites. *FEMS Microbiol Lett* 229:203–209. [https://doi.org/10.1016/S0378-1097\(03\)00822-X](https://doi.org/10.1016/S0378-1097(03)00822-X).
  48. Franco E, Vazquez-Prado J, Meza I. 1997. Fibronectin-derived fragments as inducers of adhesion and chemotaxis of *Entamoeba histolytica* trophozoites. *J Infect* 6:1597–1602. <https://doi.org/10.1086/514160>.
  49. Ravdin JI, Guerrant RL. 1981. Role of adherence in cytopathogenic mechanisms of *Entamoeba histolytica*. *J Clin Invest* 68:1305–1313. <https://doi.org/10.1172/jci110377>.
  50. Lee J, Park S-J, Yong T-S. 2008. Effect of iron on adherence and cytotoxicity of *Entamoeba histolytica* to CHO cell monolayers. *Korean J Parasitol* 46:37–40. <https://doi.org/10.3347/kjp.2008.46.1.37>.
  51. National Research Council. 2011. Guide for the care and use of laboratory animals, 8th ed. National Academies Press, Washington, DC.
  52. Ventura-Juarez J, Campos-Rodríguez R, Tsutsumi V. 2002. Early interactions of *Entamoeba histolytica* trophozoites with parenchymal and inflammatory cells in the hamster liver: an immunocytochemical study. *Can J Microbiol* 48:123–131. <https://doi.org/10.1139/w01-136>.
  53. Munro BH. 1971. Manual of histologic staining methods of the Armed Forces Institute of Pathology. *Pathology* 3:249. [https://doi.org/10.1016/S0031-3025\(16\)39410-7](https://doi.org/10.1016/S0031-3025(16)39410-7).